JOURNAL OF SOLID STATE CHEMISTRY 62, 47–56 (1986)

Heat Capacity and Thermodynamic Functions of $LuFe_2H_{2.41}$ and $ErFe_2H_{2.41}$

K. M. WISE AND R. A. BUTERA[1]

Department of Chemistry, University of Pittsburgh, Pittsburgh, Pennsylvania 15260

Received June 21, 1985; in revised form August 1, 1985

The heat capacities of $LuFe_2H_{2.41}$ and $ErFe_2H_{2.41}$ have been experimentally determined from 1.5 to 300 K. The smoothed heat capacity and thermodynamic functions ($H_T^0 - H_0^0$) and S_T^0 are reported for the two compounds. The entropy of formation of the hydride from the parent intermetallic compound is reported for both materials and for the case of the Er compound a comparison with the literature value estimated from pressure–composition measurements is made.

Introduction

The work reported in this paper is a continuation of a program to determine the thermodynamic functions which characterize rare earth–transition metal intermetallics and their hydrides. Germano *et al.* (*1*) have determined the thermodynamic functions, and crystal field contribution to the heat capacity, for a series of $REFe_2$ intermetallic compounds. In this paper we report the results of a heat capacity investigation of the hydrides of two members of this series, $LuFe_2H_{2.41}$ and $ErFe_2H_{2.41}$.

$LuFe_2$ and $ErFe_2$ crystallize in the C15 "Laves-phase," or $MgCu_2$, structure. In this structure, the rare earth atoms form a diamond structure with tetrahedra of iron atoms occupying four of the tetrahedral locations within the unit cell. Within this structure there are three different types of crystallographic sites available for hydrogen occupancy (*2*). Table I summarizes the number, type, and nearest neighbor site information. There has been interest in determining the location of the hydrogen within these sites as a function of the hydrogen content. In this regard it is to be noted that the highest concentration of hydrogen attained for these materials has been not in excess of six hydrogen atoms per formula unit of the $REFe_2$ intermetallic. Thus not all of the available sites can be occupied simultaneously. The assumption (*3*) that no two face-sharing tetrahedral sites can be simultaneously occupied, yields a maximum theoretical composition of $REFe_2H_6$. Neutron diffraction investigations of several Laves phase compounds indicate that the *g* sites are preferentially occupied at hydrogen compositions less than six per formula unit (*4*, *5*).

We have undertaken this investigation of the heat capacity in order to determine the entropy of hydride formation as a function of hydrogen content. This information will

[1] To whom all correspondence should be addressed.

0022-4596/86 $3.00

TABLE I

POSSIBLE HYDROGEN SITES IN THE C15 STRUCTURE

Wyckoff notation	Sites/unit cell	Nearest neighbors
g	96	4 RE
e	32	2 RE, 2 Fe
b	8	4 Fe

provide accurate entropy values to compare with the predictions of the various models presently being pursued in an attempt to understand the factors which govern hydride formation.

Sample Preparation

The unhydrided $ErFe_2$ sample used to prepare the $ErFe_2H_{2.41}$ was the same sample used by Germano *et al.* (*1*). The $ErFe_2$ sample used to prepare the hydrided sample for use in 1.5–16 K calorimeter and the $LuFe_2$ starting material were prepared and supplied by Ames Laboratory.

The hydrogen pressure–composition isotherms were determined for $ErFe_2H_x$ over the range $x = 1.9$ to 3.4 and for $LuFe_2H_x$ over the range $x = 2.3$ to 2.6. The data for $ErFe_2$ agrees with that reported by Kierstead (*6*). The composition corresponding to $x = 2.41$ lies in the center of a single phase region and was chosen for this study. The hydriding process induces a 5% volume expansion and results in the fracturing of the samples into a powdered form. The hydrided samples were subjected to a 30 psi atmosphere of SO_2 for a period of 2 hr to poison the surface of the hydride thus preventing subsequent loss of hydrogen. This method of protecting hydrides from hydrogen loss has been used previously in this laboratory for samples such as $LaNi_5H_7$ which has a room temperature equilibrium hydrogen vapor pressure of greater than 1 atm. In this work we have determined the suitability of the SO_2 process by subjecting a portion of the samples to the vacuum produced by a Terpler pump and found that the samples had to be heated to temperatures greater than 100°C before significant hydrogen loss was detected. The integrity of the samples was further tested by X-ray diffraction before and after the heat capacity measurements. The lattice parameters of the hydrided intermetallic are very sensitive to hydrogen content so that hydrogen loss during the calorimetric experiments would produce a decrease in the lattice parameters. The X-ray diffraction results were identical for the material before and after the calorimetric experiment and thus we conclude that hydrogen loss did not occur during the calorimetric determinations.

The samples used to determine the heat capacity over the range 10 to 300 K were directly inserted into the sample holder of the calorimeter and sealed under a He atmosphere to provide the necessary thermal contact to the calorimeter. The hydrided samples had to be prepared by a different manner in order to determine the heat capacity over the region 1.5 to 16 K as encapsulation using He exchange gas was not practical. The necessary thermal contact was obtained by mixing the hydrided material with 200 mesh copper powder (*7*) in a mass ratio of 2/1, copper/hydride, and compressing into a pellet in a stainless steel die under a 16000 psi pressure.

X-ray diffraction was used to confirm that the hydrided samples consisted of a single phase, and for the case of the compressed pellets no hydrogen was lost during the compression as evidenced by the observance of no change in the lattice parameter when compared to the uncompressed material. The lattice parameters for the samples used in this work were determined to be $a_0 = 7.73$ and 7.64 Å for $ErFe_2H_{2.41}$ and $LuFe_2H_{2.41}$, respectively. The uncertainties in the composition value have been determined to be ± 0.01.

Apparatus

Two computer controlled calorimeters were used in this study. A small sample pulse calorimeter was used to cover the temperature region 1.5 to 16 K and an adiabatic calorimeter was used to cover the temperature region 10 to 300 K.

The computer controlled adiabatic calorimeter used in this work has been described in detail by Germano (*1*), however, a brief description will be given here. The sample temperature was monitored by a four-wire platinum resistance thermometer (Leeds and Northroup 1782427) using the IPTS-68 temperature scale. Thermometer current was fixed by a constant-current supply at 10 mA for $T < 50$ K and 5 mA for $T > 50$ K. Each temperature–time datum, $T(t)$, was calculated from forty pairs of voltage/current readings (noise, signal + noise). The noise was subtracted and the signals were averaged. Those which fell outside of two standard deviations were discarded and the average was recalculated. If the number of readings retained by this process was less than 30, the datum was rejected. The temperature drift data consisted of 20 consecutive values of temperature vs time. The drift data are extrapolated back to the center of the previous heating period and forward to the center of the next heating period to allow calculation of the final and initial temperatures, respectively. In order to detect when the calorimeter had equilibrated after a heating period (i.e., the drifts are linear), the 20 $T(t)$ data were fit with linear and quadratic least squares and the root mean square (RMS) deviations were compared. When these data indicated a linear variation with time, the data were used to calculate the drift. However, if the linearity was not within acceptable limits, the calorimeter had not yet come to equilibrium. The first $T(t)$ datum was then discarded and the system acquired additional readings to calculate a new $T(t)$ datum. This method corresponds to a "walking" least squares and the process was continued until the curvature criterion was met or a specified limit on the total number of data points was exceeded. The latter case was used as an indicator of either a problem with the calorimeter or the occurrence of a process having an extremely long equilibrium time. The heating periods were 600 sec in duration with the current selected so as to provide either a constant ΔT mode or a variable ΔT mode. In the latter, ΔT was adjusted to a value of $T/10$ for $T \leq 50$ K and to a value of 5 K for $T > 50$ K. Heater voltage and current readings were taken every 0.2 sec throughout the heating period to determine the energy input. The accuracy of the calorimeter was determined using a 63.000-g sample of copper obtained from the NBS. The deviation of the experimentally determined values of the copper heat capacity from that published by the NBS is shown in Fig. 1.

A complete description of the pulse calorimeter is currently in preparation and a brief description will be given here. The calorimeter was operated in a quasiisothermal mode under computer control. The sample and sample platform are suspended from a comparably massive gold-plated copper shield (150 g) by superconducting NbZr lead wires (T_c = 14 K). The sample and shield were alternately heated so that the shield was hot with respect to the sample by $\frac{1}{2}\ \Delta T$ for the foredrift period and cold with respect to the sample by $\frac{1}{2}\ \Delta T$ for the after drift period. The shield temperature was chosen to yield the symmetrical sample temperatures with respect to the shield described above by anticipating the temperature change for the sample based on the previous heat capacity data point. Thus, the small heat leak between the sample and shield was nearly balanced over the heat capacity measurement cycle. The sample thermometry was based on a germanium resistance thermometer having a nominal re-

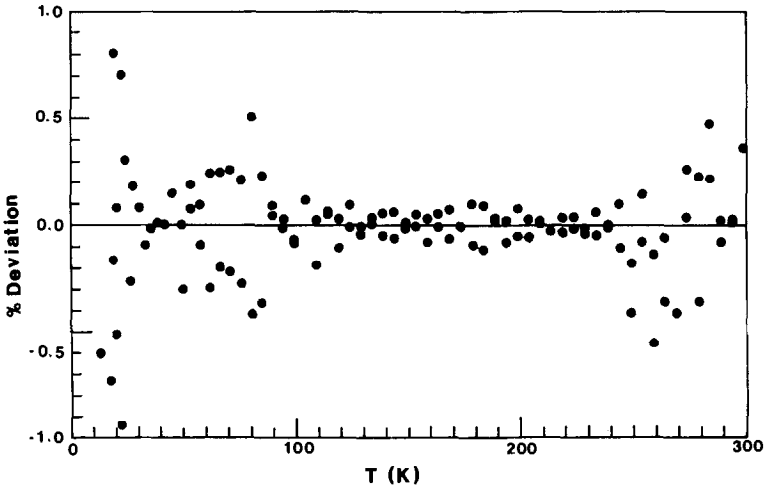

FIG. 1. Deviation of the experimental copper heat capacity values obtained using the adiabatic calorimeter from the published NBS values.

sistance of 1000 Ω at 4 K. This thermometer was calibrated using secondary standards maintained by the manufacturer (*8*). A typical temperature step size was *T*/20, although a constant heating period current mode was often used when measuring the heat capacity associated with a λ transition. The accuracy of this calorimeter has been determined using a 3.000-g sample of the same NBS copper sample used for the adiabatic calorimeter described above. The deviation of the experimentally determined values of the copper heat capacity from that published by the NBS is shown in Fig. 2.

Results and Discussion

Figures 3 and 4 show the experimental

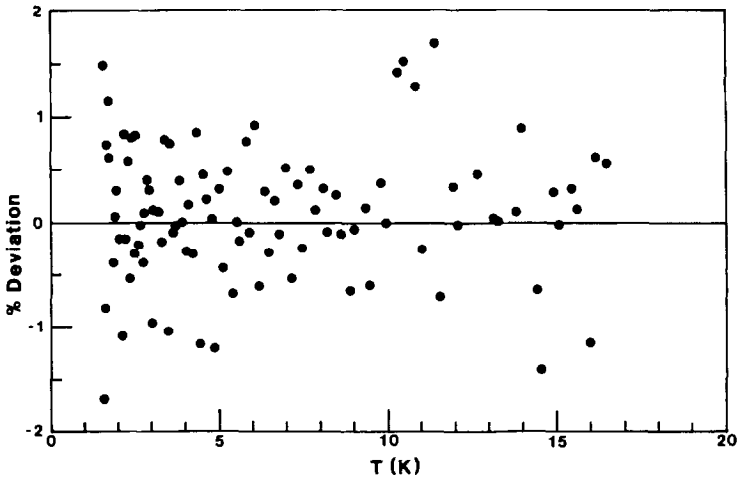

FIG. 2. Deviation of the experimental copper heat capacity values obtained using the pulse calorimeter from the published NBS values.

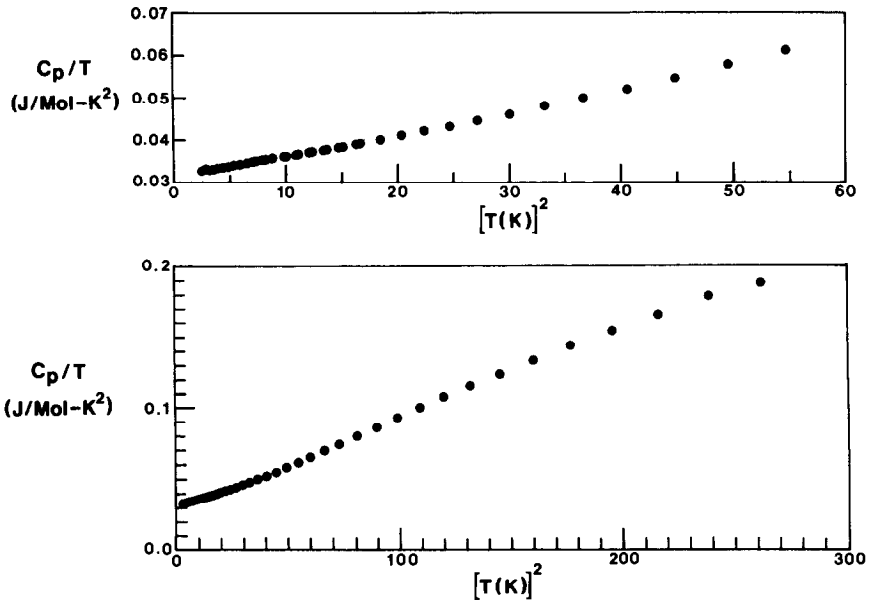

FIG. 3. Heat capacity of $LuFe_2H_{2.41}$ obtained using the pulse calorimeter.

heat capacity data[2] for $LuFe_2H_{2.41}$. The data for temperatures below 5.5 K were used to determine the electronic and lattice heat capacity coefficients γ and β using (*9*)

$$C_e = (\pi^2/3)k_B^2 T g(e_F) = \gamma T$$

$$C_l = (12\pi^4/5)R(T/\theta_D)^3 = \beta T^3$$

$$C_{total} = \gamma T + \beta T^3$$

and a least-squares fitting procedure to yield the values

$$\gamma = (0.03113 \pm 0.00006)\ \text{J/K}^2 \cdot \text{mole}$$

and

$$\beta = (0.000479 \pm 0.000004)\ \text{J/K}^4 \cdot \text{mole}.$$

The Debye temperature as derived from the value of β is

$$\theta = (230.0 \pm 0.7)\ \text{K}.$$

The values for $LuFe_2$ determined by Clinton (*10*) are

$$\gamma = (0.0128 \pm 0.0001)\ \text{J/K}^2 \cdot \text{mole}$$

$$\beta = (0.000220 \pm 0.00003)\ \text{J/K}^4 \cdot \text{mole}$$

and

$$\theta = 298\ \text{K}.$$

Comparison of these results show that γ for the hydride is larger than γ for the parent compound indicating an increase in the density of states at the Fermi level upon hydriding. The decrease in the Debye temperature upon hydriding indicates that the introduction of hydrogen into the structure reduces the lattice stiffness.

[2] See NAPS document 04349 for 6 pages of supplementary material. Order from ASIS/NAPS, Microfiche Publications, P. O. Box 3513, Grand Central Station, New York, N.Y. 10163. Remit in advance $4.00 for microfiche copy or for photocopy, $7.75 up to 20 pages plus $0.30 for each additional page. All orders must be prepaid. Institutions and organizations may order by purchase order. However, there is a billing and handling charge for this service of $15. Foreign orders add $4.50 for postage and handling, for the first 20 pages, and $1.00 for additional 10 pages of material. $1.50 for postage of any microfiche orders.

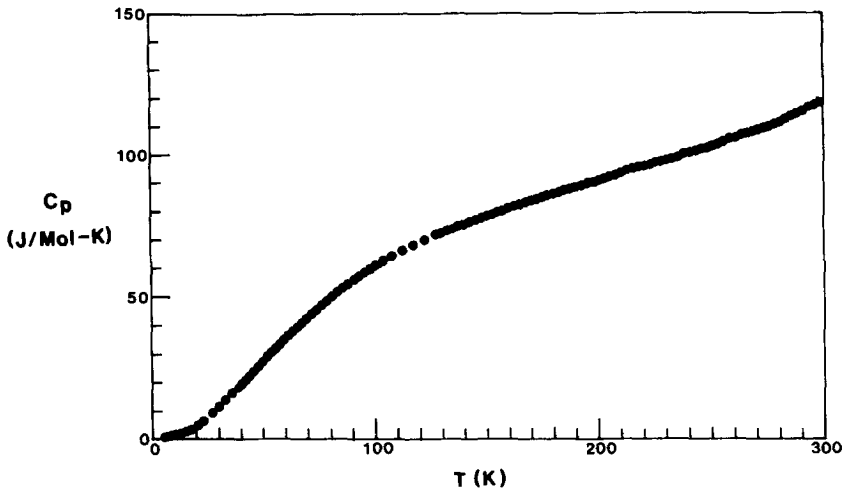

FIG. 4. Heat capacity of $LuFe_2H_{2.41}$ obtained using the adiabatic calorimeter.

The data obtained using both calorimeters were combined and smoothed using mechanical splines from 5.5 to 295 K. Below 5.5 K the expression

$$C_p\ [\text{J/K} \cdot \text{mole}] = 0.03113T + 0.000479T^3$$

was used to obtain the smoothed values. The smoothed heat capacity and thermodynamic functions $(H_T^0 - H_0^0)$ and S_T^0 for $LuFe_2H_{2.41}$ are given in Table II. Combining these results with the heat capacity data for $LuFe_2$ (*1, 10, 11*) yield the following differences:

$$[H^0(285) - H^0(0)]_{hyd} - [H^0(285) - H^0(0)]_{met} = 4384\ \text{J/mole},$$

$$[S^0(285) - S^0(0)]_{hyd} - [S^0(285) - S^0(0)]_{met} = 31.3\ \text{J/mole} \cdot \text{K}.$$

Figures 5–7 show the experimental heat capacity data for $ErFe_2H_{2.41}$. The data for temperatures below 5 K exhibit a peak centered at 3.4 K and a upturn of the heat capacity for temperatures below 2 K. In order to determine the source of the anomaly centered at 3.4 K we have determined the heat

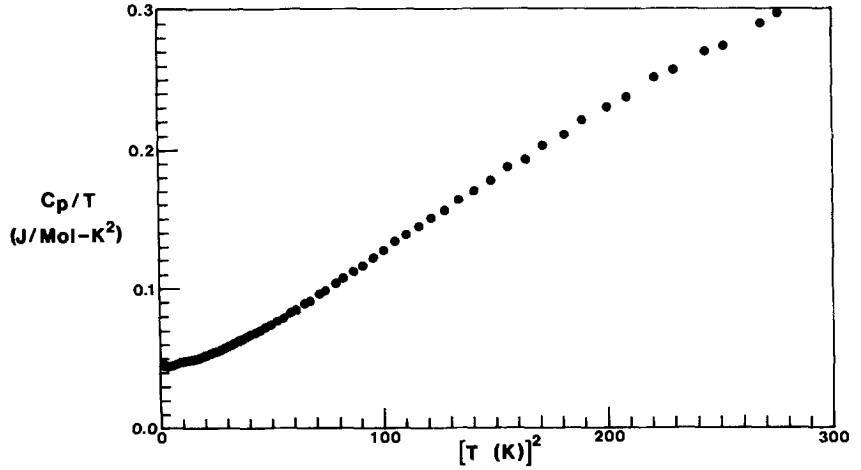

FIG. 5. Heat capacity of $ErFe_2H_{2.41}$ obtained using the pulse calorimeter.

TABLE II

SMOOTH THERMODYNAMIC FUNCTIONS OF $LuFe_2H_{2.41}$

T (K)	C_p (J/mole · K)	$H_T^0 - H_0^0$ (J/mole)	$S_T^0 - S_0^0$ (J/mole · K)
1.5	0.049	0.035	0.047
2.0	0.066	0.064	0.064
3.0	0.106	0.150	0.098
4.0	0.154	0.279	0.135
5.0	0.216	0.463	0.175
6.0	0.297	0.717	0.222
7.0	0.404	1.065	0.275
8.0	0.542	1.535	0.337
9.0	0.716	2.161	0.411
10.0	0.930	2.981	0.497
15.0	2.550	11.336	1.153
20.0	4.975	29.810	2.199
30.0	11.67	111.49	5.42
40.0	19.49	266.74	9.83
50.0	27.58	501.46	15.04
60.0	35.41	816.79	20.76
70.0	42.76	1208.10	26.78
80.0	49.61	1670.45	32.94
90.0	55.74	2198.13	39.15
100.0	60.84	2781.93	45.30
110.0	65.14	3412.37	51.30
120.0	68.88	4082.81	57.14
130.0	72.29	4788.92	62.79
140.0	75.41	5527.61	68.26
150.0	78.33	6296.40	73.56
160.0	81.07	7093.52	78.71
170.0	83.63	7917.09	83.70
180.0	86.09	8765.77	88.55
190.0	88.53	9638.87	93.27
200.0	90.97	10536.4	97.87
210.0	93.38	11458.0	102.37
220.0	95.81	12404.0	106.77
230.0	98.23	13374.1	111.08
240.0	100.69	14368.7	115.31
250.0	103.23	15388.2	119.47
260.0	105.86	16433.4	123.57
270.0	108.64	17505.7	127.62
280.0	111.85	18607.8	131.63
290.0	115.47	19743.9	135.61
295.0	117.44	20326.2	137.60

capacity of Er_2O_3 and the results are shown in Fig. 8. The data reported by Westrum *et al.* (*12*) are also shown for comparison. The oxide heat capacity exhibits a strong λ anomaly at 3.4 K corresponding to the onset of magnetic ordering in this material. These data were used to eliminate the anomaly in the hydride data associated with a small oxide impurity. The upturn of the heat capacity of the hydride occuring below 2 k has been attributed to the onset of the nuclear hyperfine contribution to the heat capacity. The excess heat capacity associated with the hyperfine interaction has been fit using the hyperfine interaction parameter $a' = 0.0471$ and the natural abundance of the Er^{167} isotope of 22.94% with a nuclear spin of $I = \frac{7}{2}$. The hyperfine contribution was subtracted from the data and then the oxide data were scaled and subtracted so as to linearize the data below 6.5 K. Figure 9 shows the result of subtracting the oxide and hyperfine contributions. The data below 6.5 K were fit by linear least squares yielding the following values for the hydride

$$\lambda = (0.03574 \pm 0.00008) \text{ J/mole} \cdot \text{K}^2$$

$$\beta = (0.000724 \pm 0.000004) \text{ J/mole} \cdot \text{K}^4$$

and

$$\theta_D = (200.4 \pm 0.4) \text{ K}.$$

The values for $ErFe_2$ determined by Clinton (*11*) are

$$\gamma = (0.0132 \pm 0.0002) \text{ J/mole} \cdot \text{K}^2$$

$$\beta = (0.000223 \pm 0.000003) \text{ J/mole} \cdot \text{K}^4$$

and

$$\theta_D = 297 \text{ K}.$$

Comparison of these results shows that γ for the hydride is larger than that for the

TABLE III

LATTICE CONSTANTS AND DEBYE TEMPERATURES

Compound	Lattice constant (Å)	θ_D	a_0(hyd)/a_0(met)
$LuFe_2H_{2.41}$	7.64	230.0	1.059
$LuFe_2$	7.217	298	
$ErFe_2H_{2.41}$	7.73	200.4	1.062
$ErFe_2$	7.280	297	

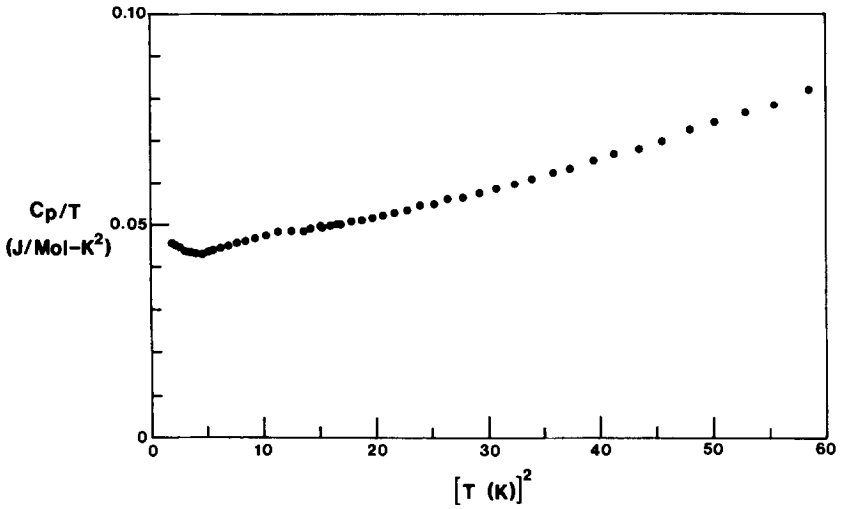

FIG. 6. Heat capacity of $ErFe_2H_{2.41}$ obtained using the pulse calorimeter, expansion of low temperature region.

parent compound indicating an increase in the density of states at the Fermi level similar to that observed for $LuFe_2H_{2.41}$. However the decrease in θ_D upon hydriding is larger than that observed for $LuFe_2H_{2.41}$. The difference in the effect on θ_D is difficult to interpret as the percent lattice expansion is nearly the same for both materials (Table III).

The data obtained using both calorimeters were combined, corrected for the oxide contribution, and smooth values for the heat capacity below 7 K were obtained by adding the calculated C_l, C_e, and C_n. Mechanical splines were used to smooth the data from 7 to 300 K. The smoothed heat capacity and thermodynamic functions ($H_T^0 - H_0^0$) and S_T^0 for $ErFe_2H_{2.41}$ are given in

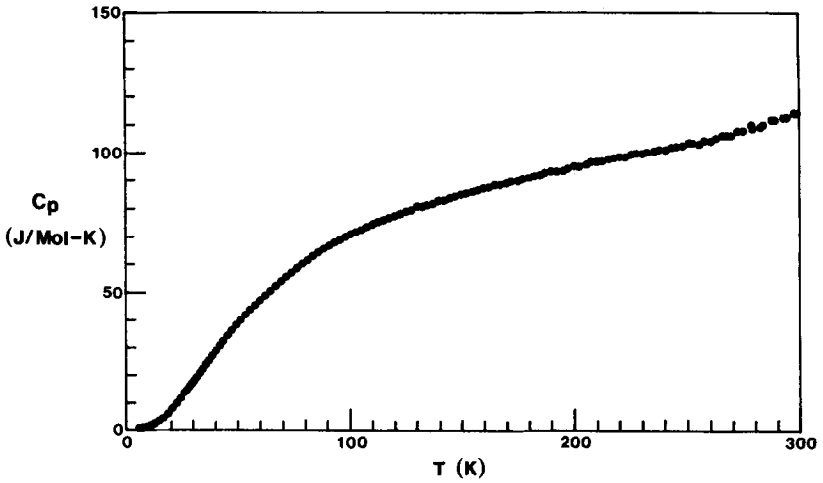

FIG. 7. Heat capacity of $ErFe_2H_{2.41}$ obtained using the adiabatic calorimeter.

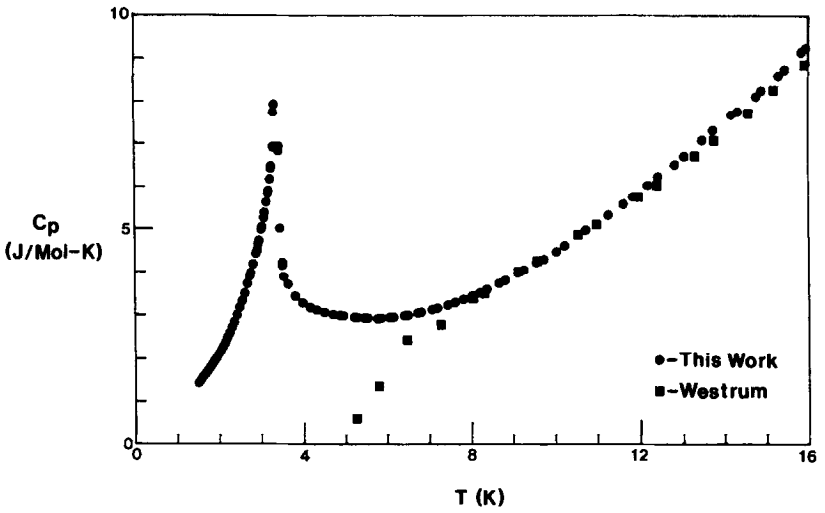

FIG. 8. Low temperature heat capacity of Er_2O_3.

Table IV. Combining these results with the heat capacity data for $ErFe_2$ (*1*, *11*) yield the following differences:

$$[H^0(285) - H^0(0)]_{hyd} - [H^0(285) - H^0(0)]_{met} = 3615 \text{ J/mole},$$

$$[S^0(285) - S^0(0)]_{hyd} - [S^0(285) - S^0(0)]_{met} = 30.86 \text{ J/mole} \cdot \text{K}.$$

Kerstead (*6*) has reported the entropy of hydride formation derived from pressure–composition isotherms and a comparison with our data yield

Kerstead: $[S^0(283.15)]_{hyd} - [S^0(283.15)]_{met} = 29.3$ J/mole · K,

and

this work: $[S^0(283.15)]_{hyd} - S^0(283.15)]_{met} = 30.70 \pm 0.85$ J/mole · K.

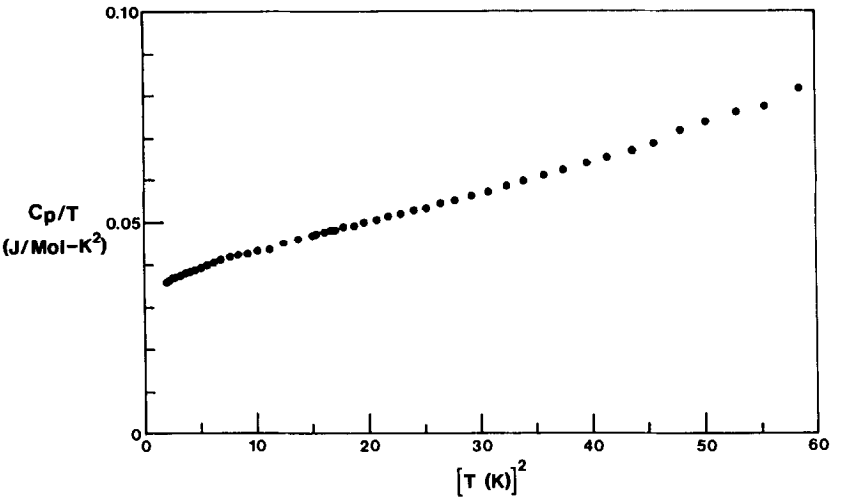

FIG. 9. Low temperature heat capacity of $ErFe_2H_{2.41}$ corrected for nuclear and oxide contributions.

TABLE IV

SMOOTH THERMODYNAMIC FUNCTIONS FOR $ErFe_2H_{2.41}$

T (K)	C_p (J/mole · K)	$H_T^0 - H_0^0$ (J/mole)	$S_T^0 - S_0^0$ (J/mole · K)
1.5	0.066	0.041	4.016
2.0	0.083	0.078	4.037
3.0	0.129	0.183	4.079
4.0	0.191	0.341	4.124
5.0	0.270	0.570	4.174
6.0	0.372	0.888	4.232
7.0	0.513	1.327	4.300
8.0	0.703	1.931	4.380
9.0	0.951	2.752	4.476
10.0	1.264	3.854	4.592
15.0	3.772	1.578	5.525
20.0	7.722	44.010	7.122
30.0	17.84	169.96	12.09
40.0	28.72	403.49	18.73
50.0	38.94	742.59	26.26
60.0	46.98	1173.72	34.10
70.0	54.30	1680.44	41.89
80.0	60.99	2257.63	49.59
90.0	66.48	2896.14	57.11
100.0	70.82	3583.59	64.34
110.0	74.61	4311.23	71.28
120.0	77.73	5073.55	77.91
130.0	80.38	5864.36	84.23
140.0	82.78	6680.30	90.28
150.0	85.02	7519.49	96.07
160.0	87.14	8380.48	101.63
170.0	89.13	9261.77	106.97
180.0	91.07	10162.8	112.12
190.0	92.98	11083.0	117.09
200.0	94.89	12022.5	121.91
210.0	96.72	12980.6	126.59
220.0	98.45	13956.4	131.13
230.0	100.10	14949.3	135.54
240.0	100.89	15451.8	137.70
250.0	103.16	16982.2	144.01
260.0	104.73	18021.5	148.09
270.0	106.72	19078.3	152.08
280.0	109.22	20157.7	156.00
290.0	112.10	21264.0	159.88
300.0	115.47	22401.5	163.74

Considering the uncertainty in extracting the entropy values from pressure–composition isotherms due to the need to extrapolate the data below $x = 1$ and the cross-plotting required, the values obtained from the calorimetric data are to be considered not in disagreement and of higher accuracy.

As can be seen in Figs. 4 and 9, the heat capacity of both materials tend to rise with temperature above 250 K. This can be attributed to the fact that both materials magnetically disorder near 500 K and the rise in the heat capacity is associated with the approach to the critical magnetic transition.

References

1. D. J. GERMANO, R. A. BUTERA, AND K. A. GSCHNEIDNER, JR., *J. Solid State Chem.* **37,** 389 (1981); D. J. GERMANO AND R. A. BUTERA, *Phys. Rev. B 1,* **24,** 3912 (1981); also D. J. GERMANO, Ph. D. Thesis, University of Pittsburgh (1980).
2. "International Tables for X-Ray Crystallography," Kynoch Press, Birmingham (1965).
3. C. B. SHOEMAKER AND D. P. SHOEMAKER, *J. Less Common Met.* **64,** 43 (1979).
4. J. DIDISHEIM, K. YUON, D. SHALTIEL, AND P. FISCHER, *Solid State Commun.* **31,** 47 (1979).
5. J. DIDISHEIM, K. YUON, D. SHALTIEL, P. FISCHER, P. BUJARD, AND E. WALKER, *Solid State Commun.* **32,** 1087 (1979).
6. H. A. KIERSTEAD, *J. Less Common. Met.* **70,** 199 (1980).
7. Alpka-Thiokol Chemicals, 200 mesh, 99.99% copper powder.
8. Germanium resistance thermometer, CryoCal, Inc., Riviera Beach, Fla. 33404.
9. N. W. ASHCROFT AND N. W. MERMIN, "Solid State Physics," McGraw–Hill, New York (1965).
10. R. A. Butera, T. J. Clinton, A. G. Moldovon, S. G., Sankar, and K. A. Gschneidner, Jr., *J. Appl. Phys.* **50,** 7492 (1979).
11. T. J. CLINTON, Ph.D. thesis, University of Pittsburgh (1981).
12. E. F. WESTRUM AND B. H. JUSTICE, *J. Phys. Chem.* **67,** 659 (1963).